

Paraoxonase 2 attenuates macrophage triglyceride accumulation via inhibition of diacylglycerol acyltransferase 1

Mira Rosenblat,* Raymond Coleman,[†] Srinivasa T. Reddy,[§] and Michael Aviram^{1,*}

Lipid Research Laboratory,* Technion Faculty of Medicine, Rappaport Family Institute for Research in the Medical Sciences, Rambam Medical Center, Haifa, Israel; Department of Anatomy and Cell Biology,[†] Technion Faculty of Medicine, Haifa, Israel; and Atherosclerosis Research Unit,[§] Division of Cardiology, Department of Medicine, University of California, Los Angeles, CA 90095-1679

Abstract This study questioned the role of paraoxonase 2 (PON2) in attenuation of macrophage lipids accumulation. Mouse peritoneal macrophages (MPMs) harvested from PON2-deficient mice versus control C57BL/6 mice, look like foam cells and were larger in size and filled with lipid droplets. Macrophage triglyceride (but not cholesterol) content, biosynthesis rate, and microsomal acyl-CoA:diacylglycerol acyltransferase 1 (DGAT1) activity (not mRNA and protein) in PON2-deficient versus control MPM were all significantly increased by 4.6-, 3.6-, and 4.4-fold, respectively. Similarly, microsomal DGAT1 activity and cellular triglyceride content were significantly decreased in human PON2-transfected cells as well as upon incubation of PON2-deficient MPM with recombinant PON2. In all the above experimental systems, PON2 also decreased macrophage oxidative state. Incubation of PON2-deficient MPM with the free radicals generator 2,2'-amidinopropane hydrochloride increased cellular oxidative stress and DGAT1 activity by 2.2- and 3.4-fold, respectively, whereas incubation of microsomes from PON2-deficient MPM with superoxide dismutase decreased DGAT1 activity by 40%. We thus conclude that PON2 attenuates macrophage triglyceride accumulation and foam cell formation via inhibition of microsomal DGAT1 activity, which appears to be sensitive to oxidative state.—Rosenblat, M., R. Coleman, S. T. Reddy, and M. Aviram. **Paraoxonase 2 attenuates macrophage triglyceride accumulation via inhibition of diacylglycerol acyltransferase 1.** *J. Lipid Res.* 2009. 50: 870–879.

Supplementary key words macrophages • triglycerides • oxidative stress

Cholesterol and triglycerides are independent risk factors for atherosclerosis (1, 2). One of the earliest events during the development of atherosclerotic lesions is the accumulation of lipid-laden macrophages in the artery wall (3–5). Atherosclerotic lesions, as well as macrophages isolated from lesions, contain predominantly cholesterol

esters but also substantial amount of triglycerides (6–8). Triglyceride-rich lipoproteins were suggested to contribute to foam cell formation through a local degradation of these lipoproteins by lipoprotein lipase and a subsequent uptake of the remnant particles into macrophages (9, 10). Triglyceride accumulation in macrophages results in an increased oxidative stress (11), thus further contributing to foam cell formation.

Mammalian paraoxonases (PON1, PON2, and PON3) are a unique family of calcium-dependent hydrolases (12), with enzymatic activities toward a broad range of substrates (lactones, thiolactones, carbonates, esters, and phosphotriesters). Although the physiological substrates of PONs were not identified yet, several studies suggest that they could be lipolactones, specific oxidized phospholipids, products of enzymatic and nonenzymatic oxidation of arachidonic and docosahexaenoic acid, and *N*-acyl-homoserine lactones. Unlike PON1, which is present in serum as HDL-associated enzyme, PON2 is not detectable in serum. Whereas PON1 is expressed mainly in the liver, PON2 is expressed in most tissues, including macrophages (13, 14). In hypercholesterolemic patients, decreased macrophage PON2 expression was noted (15), and PON2 expression in human carotids was shown to be decreased during the progression of atherosclerosis (16). PON2, like PON1, was shown to protect against atherosclerosis development (17, 18), and this could be related to PON2 ability to inhibit cell-mediated LDL oxidation, oxidized LDL (OxLDL)-induced monocytes chemotaxis, and formation of reactive oxygen species (ROS) (13, 14, 19). Macrophage oxidative stress was shown to affect PON2 expression and activities in a biphasic U-shape pattern (14, 20). Upregulation

Abbreviations: AAPH, 2,2'-amidinopropane hydrochloride; DGAT1, acyl-CoA:diacylglycerol acyltransferase 1; hPON2, human paraoxonase 2; MPM, mouse peritoneal macrophage; oxLDL, oxidized low density lipoprotein; PON, paraoxonase; SOD, superoxide dismutase.

¹To whom correspondence should be addressed.

e-mail: aviram@tx.technion.ac.il

Manuscript received 27 October 2008 and in revised form 10 December 2008.

Published, JLR Papers in Press, December 16, 2008.

DOI 10.1194/jlr.M800550-JLR200

of macrophage PON2 was shown to occur via several mechanisms, including NADPH-oxidase activation (21), pomegranate juice polyphenolic antioxidants (22), unesterified cholesterol accumulation (23), and urokinase plasminogen activator (24).

Macrophage atherogenicity is defined by increased cellular oxidative stress as well as lipid accumulation. Macrophage PON2 was shown to reduce cellular oxidative stress (24), but no data exist on the effect of PON2 on macrophage lipid accumulation. Thus, our goal was to analyze a possible role of PON2 (and mechanism of action) in protecting macrophages from specific lipid accumulation.

MATERIALS AND METHODS

Generation of PON2-deficient mice

The PON2-deficient mice on the C57BL/6 background were generated as previously described (18). The mice were fed with chow diet. The weight of the PON2-deficient mice (5 months old) was increased by 23% compared with the weight of age-matched control mice (38.1 ± 2.3 versus 30.9 ± 1.3 g, respectively, $n = 6$). The weight of (5 months old) PON2-deficient mice livers was increased by 64% compared with the livers obtained from control mice (2.42 ± 0.1 g versus 1.48 ± 0.48 g, respectively). The PON2-deficient mice and C57BL/6 mice were obtained from the UCLA lab. The animal experimentation was performed in the Technion Faculty of Medicine. We used only male mice in our study. The research was conducted in conformity with the Public Health Service Policy on Human Care and Use of Laboratory Animals. The studies were approved by the Committee for Supervision of Animal Experiments, the Technion- Israel Institute of Technology, Haifa.

Mouse peritoneal macrophages

Mouse peritoneal macrophages (MPMs) were harvested from the peritoneal fluid of 10 control (C57BL/6) mice or from 10 PON2-deficient mice, 4 days after intraperitoneal injection into each mouse of 3 ml of aged thioglycolate (40g/l) in saline. The cells ($10\text{--}20 \times 10^6$ /mouse) were washed and centrifuged three times with PBS at 1,000 *g* for 10 min and then resuspended at 10^9 /liter in DMEM containing 5% fetal calf serum, 1×10^5 units penicillin/liter, 100 mg streptomycin/liter, and 2 mmol/liter glutamine. The dishes were incubated in a humidified incubator (5%CO₂, 5% air) for 2 h and washed with DMEM to remove non-adherent cells, and the analyses to measure cellular oxidative stress were immediately performed.

Histological analysis of the mice MPM

The macrophage pellets from C57BL/6 control mice or from PON2-deficient mice at the age of 5 months were fixed in 3% glutaraldehyde in 0.1 M sodium cacodylate buffer, pH 7.4, overnight. They were rinsed and stored in the 0.1 M cacodylate buffer with 7.5% sucrose followed by 1% osmium tetroxide in water (1 h), dehydration in graded ethanols (70, 95, and 100%), cleared in propylene oxide, and embedded in Epon resin (Eponate 12; Ted Pella, Redding, CA). The resin was polymerized overnight at 60°C. Blocks were cut on an ultramicrotome with a diamond knife, and the 1 μ m thick sections were stained with 0.1 toluidine blue in 1% borax (sodium tetraborate). The sections were photographed with an Olympus C5060W digital camera on a CH30 model Olympus bright-field microscope. The lipid in these sections has a light green color (25). Oil red O is used for staining

lipids only in fresh or frozen tissues as it is a water-based dye and is not useful for permanent slides. Oil red O is not suitable for staining lipids in fixed tissue. In our case, our tissues were fixed in buffered glutaraldehyde, and subsequently the lipid was stained with osmium tetroxide during the tissue processing. The material was embedded in Epon resin and cut very thin. This technique allows far better resolution than is possible in frozen sections stained with oil red O (25).

Transfection of MPM with human PON2

MPM from PON2-deficient mice were transfected with 2 μ g/ml of plasmid DNA [human PON2 (hPON2) gene in pcDNA3.1+ plasmid or with the empty pcDNA3.1+ plasmid, a generous gift from Dr. Dragomir Draganov, University of Michigan, Ann Arbor, MI] in Dulbecco's Modified Eagle's Medium containing 3 μ l/ml of FuGene6 reagent (Roche). The transfection reagent was removed after 4 h, followed by the addition of DMEM medium + 10% fetal calf serum. All the assays were performed 48 h after the transfection. The transfection efficiency was quantified by flow cytometry evaluation of enhanced green fluorescent protein expression in the cells, and it was found to be 60%. FuGene6 is a highly efficient transfection reagent that is useful for in vitro non-viral transfection of primary cells like human fibroblasts and rat skeletal muscle cell. In these studies, optimization of transfection conditions yielded efficiencies exceeding 50% (26, 27).

Macrophage cholesterol mass

Lipids from the mice MPM (3×10^6) were extracted with hexane:isopropanol (3:2, v: v), and the hexane phase was evaporated under nitrogen. The amount of cellular cholesterol was determined using a kit (CHOL; Roche Diagnostics, Mannheim, Germany). After extraction of cellular lipids, the cells were dissolved in 0.1 M NaOH for measurement of cellular protein by the Lowry assay (28).

Separation of cellular lipids by TLC

Lipids from the mice MPM (3×10^6) were extracted with hexane:isopropanol (3:2, v: v), and the hexane phase was evaporated under nitrogen. Chloroform was added to the dried samples, followed by their loading on silica gel 60 F₂₅₄ plates, 20 \times 20 cm (Merck; Darmstadt, Germany) and lipid separation using a mixture of 130 ml hexane, 30 ml ether, and 1.5 ml acetic acid. The separated lipids were visualized using iodine vapor.

MPM triglycerides mass

The triglycerides spots were scraped from the TLC plate, followed by lipid extraction with hexane:isopropanol (3:2, v: v), and the hexane phase was evaporated under nitrogen. The amount of cellular triglyceride in the dried samples was determined (after addition of 50 μ l DMSO) using a triglyceride determination kit (Sigma-Aldrich; catalog number TR0100). After extraction of cellular lipids, the cells were dissolved in 0.1 M NaOH for measurement of cellular protein by the Lowry assay (28).

MPM triglyceride biosynthesis

The amount of [³H]oleate incorporated into triglyceride was determined as previously described (29). Cells were incubated for 3 h at 37°C in serum-free medium containing 6 μ Ci/ml [³H]oleate bound to fatty-acid-free BSA (2%). After incubation, the cells were washed twice with PBS, pH 7.4, the lipids were extracted and separated by TLC, and the radioactivity in the bands corresponding to triglyceride was determined by liquid scintillation counting. After extraction of cellular lipids, the cells were dissolved in 0.1 M NaOH for measurement of cellular protein (28).

MPM microsome separation

Microsomes were isolated from MPM of PON2-deficient or C57BL/6 mice as previously described (10). The cells (20×10^6) were washed with cold PBS and scraped from the dishes into buffer A (50 mM Tris/HCl, pH 7.4, 250 mM sucrose, and mix protease inhibitors), followed by centrifugation for 15 min at 1,200 *g* and 4°C (to remove cell debris) and centrifugation for 15 min at 9,000 *g* (to remove mitochondria). The supernatant obtained after the second centrifugation was collected and further centrifuged at 100,000 *g* to obtain the microsome pellet. The pellet was suspended with buffer A, and the protein concentration was determined by the Bradford assay.

Acyl-CoA:diacylglycerol acyltransferase 1 mRNA expression by quantitative RT-PCR

Total RNA was extracted with an Epicentre commercial kit (Tamar, Israel). cDNA was generated from 1 µg of total RNA using a Thermo Scientific commercial kit (Tamar, Israel). Products of the reverse transcription were subjected to quantitative PCR using TaqMan gene expression assays. Quantitative PCR was performed on the Rotor-Gene 6000 system (Corbett Life Science, Australia). To normalize the data obtained for acyl-CoA: diacylglycerol acyltransferase 1 (DGAT1) expression, the amount of GAPDH mRNA was measured by quantitative PCR as internal standard in all treatments. The primers and probes for hPON2, mouse DGAT1, and GAPDH were design by Primer Design (South Hampton, UK): DGAT1 sense primer, TGGTGGAAATGCTGAGTCTG; DGAT1 antisense primer, GGTCAAAAATACTCCTGTCTCTG; DGAT1 perfect probe, CCACCCATTTGCTGCTGCCATGTCTGAggtgg; PON2 sense primer, CGACTTAAAGCCTCCAGAGAA; PON2 antisense primer, GGGAATTTTAGACCCACACTAAA; PON2 double dye TaqMan probe, TAGACCTTCCACACTGCCACCTGA.

DGAT1 protein determination by Western blot analysis

Western blot analysis was performed using SDS- PAGE and 10% Bis-acrylamide gels. Cell lysates (20 µg protein/ml) were loaded on the gel. Blocking of the gel was performed with 2% BSA for 2 h at room temperature. The primary antibody was goat polyclonal anti-human DGAT1, from Novous Biologicals [diluted 1:500 to a final concentration of 1 µg/ml, v/v, in TBS-T (5 M NaCl, 2 M Tris, pH 7.5, and Tween 20) with 0.5% BSA], and it was incubated with the nitrocellulose membrane at 4°C overnight. The secondary antibody, rabbit anti-goat horseradish-peroxidase-conjugated (Sigma-Aldrich), diluted 1:10,000 in TBS-T, was incubated for 1 h at room temperature. The membranes were developed using the ECL Western blotting kit (Amersham).

Microsomal DGAT1 activity

DGAT1 activity was determined using microsomes (30 µg protein/ml), in a total volume of 200 µl using reaction buffer (175 mM Tris/HCl, pH 8.0, 8 mM MgCl₂, and 5 mg/ml fatty-acid-free BSA) with no addition (basal microsomal triglyceride levels) or with the addition of 200 µM 1, 2-dioleoyl-glycerol and 135 µM oleoyl CoA (10). The samples were incubated for 3 h at room temperature, followed by lipid extraction and triglyceride separation by TLC. The amount of triglyceride in the TLC spots was determined using a triglyceride determination kit (Sigma-Aldrich; catalog number TR0100). DGAT1 activity is expressed as micrograms of triglyceride synthesized/milligram protein.

Macrophage lipid peroxides content

Lipids from the mice MPM (3×10^6) were extracted with hexane:isopropanol (3:2, v: v), and the hexane phase was evaporated under nitrogen. The amount of lipid peroxides in the dried

samples was measured by the method of El-Saadani et al. (30). After extraction of cellular lipids, the cells were dissolved in 0.1 M NaOH for measurement of cellular protein by the Lowry assay (28).

Statistical analyses

Each separate experiment was performed in triplicate, and each individual experiment was replicated three times ($n = 3$) to achieve statistical meaning. Statistical analyses used Student's *t*-test for comparing differences between the two groups, and one-way ANOVA followed by the Student-Newman-Keuls test was used for comparing differences between multiple groups. Results are given as mean \pm SD.

RESULTS

Lipid accumulation in macrophages from PON2-deficient mice versus control mice

We analyzed at first the effect of PON2 on cellular lipid content using peritoneal macrophages (MPM) from PON2-deficient mice versus control (C57BL/6) mice. Histological analysis of these cells as shown in **Fig. 1A, B** demonstrated that MPM from PON2-deficient mice versus control mice, at the age of 5 months, were larger and filled with lipid droplets, resembling foam cells. Indeed, upon staining the cells with alkaline toluidine blue (**Fig. 1C, D**), it can be seen that the PON2-deficient MPMs (**Fig. 1D**) accumulate significantly more lipids than the control MPM (**Fig. 1C**).

To examine which lipids accumulated in MPM from PON2-deficient mice, macrophage lipid contents were determined. Cellular total cholesterol content analysis revealed a small and nonsignificant increase, by only 12%, in PON2-deficient MPM versus control MPM (**Fig. 1E**). Upon separation of the macrophage lipids extracts by TLC, we clearly observed a significant increase in the triglyceride spot obtained from PON2-deficient MPM compared with control MPM. Indeed, a direct measurement of triglycerides in the TLC spots revealed a substantial increase, by 4.6-fold, in cellular triglyceride content of PON2-deficient MPM versus control MPM (**Fig. 1F**). Accumulation of triglycerides in PON2-deficient MPM was not cytotoxic to the cells, as lactate dehydrogenase release to the medium was minimal and similar to the lactate dehydrogenase content observed in medium from control MPM (13 ± 4 and 14 ± 3 U/mg cell protein, respectively). Accumulation of triglycerides, but not cholesterol, was also observed in aortas and in livers (the site for triglyceride biosynthesis) from PON2-deficient mice versus control mice (data not shown).

Increased triglyceride biosynthesis in macrophages from PON2-deficient versus control mice

To find out whether macrophage triglyceride accumulation in PON2-deficient MPM resulted from a possible inhibition in cellular triglyceride hydrolysis, we first incubated the cells with labeled oleic acid for 3 h, followed by cell wash, and then monitored radiolabeled triglyceride levels for a further 4 h of incubation (**Fig. 2A**). In both control MPM and PON2-deficient MPM, cellular labeled triglyceride

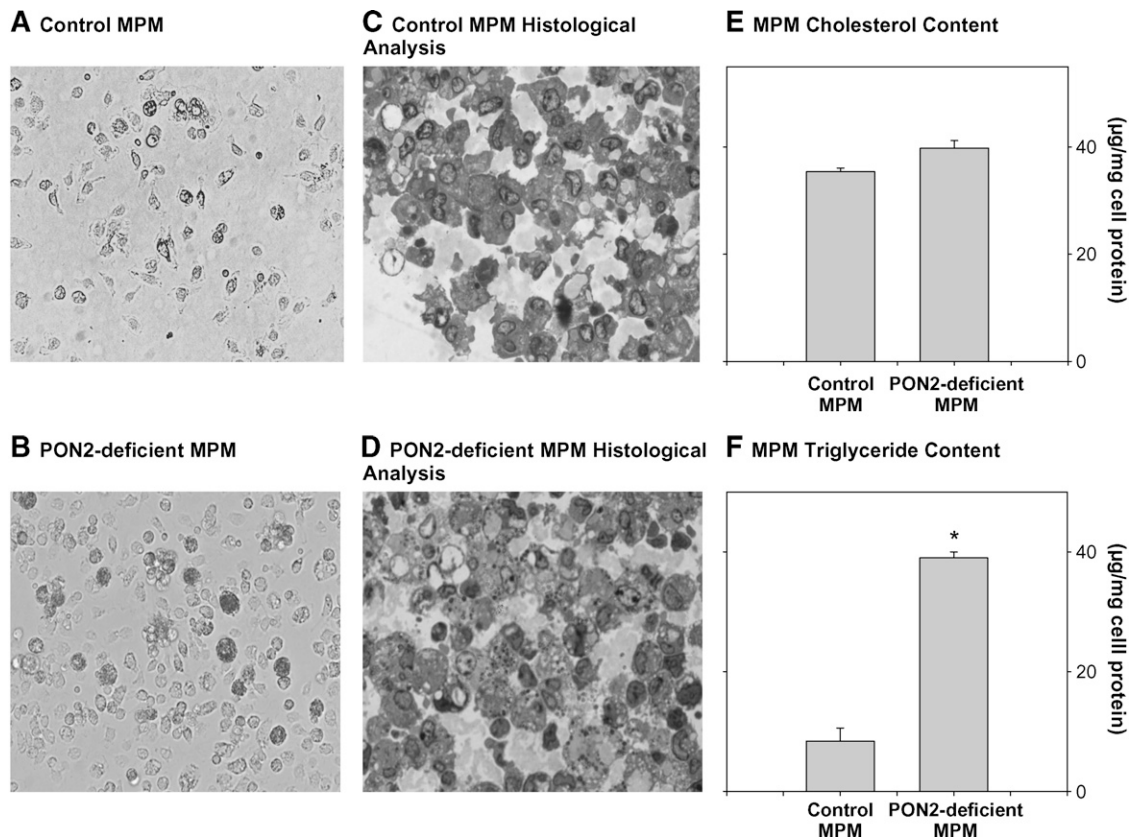


Fig. 1. Lipid accumulation in peritoneal macrophages from PON2-deficient versus control C57BL/6 mice. MPMs were harvested from 5-month-old control (C57BL/6) mice and from age matched PON2-deficient mice. A: Inverted microscopic picture of control MPM cell culture. B: Inverted microscopic picture of PON2-deficient MPM cell culture. C and D: Histological analyses of control MPM (C) and PON2-deficient MPM (D) were performed as described in Materials and Methods. E, F: The cellular lipids were extracted. E: Total cellular cholesterol content. F: The cellular lipids were separated by TLC, and the cellular triglyceride content (from the TLC spots) was determined after lipid extraction as described in Materials and Methods. Results represent mean \pm SD of 10 mice in each group. * $P < 0.01$ versus control MPM.

content decreased with time in a similar pattern (Fig. 2A). After 4 h of incubation, cellular labeled triglyceride content decreased by 56% and by 44% in PON2-deficient MPM and in control MPM, respectively, compared with levels observed at 0 time (Fig. 2A). Thus, there was no inhibition in macrophage triglycerides hydrolysis in PON2-deficient MPM.

Next, we questioned whether the accumulation of triglyceride in PON2-deficient MPM could have resulted from stimulation in cellular triglyceride biosynthesis rate. A time study was performed to measure the extent of triglyceride biosynthesis in PON2-deficient versus control MPM after 0.5, 1, 3, and 6 h of incubation (Fig. 2B). Cellular triglyceride content in both cell types gradually increased with time and reached a maximal level after 3 h of incubation. Thus, this time point was used in all our further experiments. At each time point, the level of radiolabeled triglycerides was significantly increased (by up to 3.6-fold) in PON2-deficient versus control MPM (Fig. 2B).

These results indicate that accumulation of triglycerides in PON2-deficient MPM could be related to increased triglyceride biosynthesis, but not to decreased triglyceride breakdown. To find out whether macrophage triglyceride content increases with the PON2-deficient mice age, we

harvested MPM from PON2-deficient mice (as well as from control mice) at the age of 2, 5, and 9 months. Accumulation of triglycerides in MPM from PON2-deficient mice (but not in MPM from control mice) significantly increased with the mice age up to 6.7-fold (Fig. 2C). This phenomenon could have probably been related to the increased extent of triglyceride biosynthesis by PON2-deficient versus control MPM, with the mice age. Indeed, as shown in Fig. 2D, in PON2-deficient MPM, but not in control MPM, the extent of triglyceride biosynthesis significantly increased with the mice age by up to 6-fold at the age of 9 months (Fig. 2D).

DGAT1 expression in macrophages from PON2-deficient versus control mice

DGAT1 is an endoplasmic reticulum membrane-associated enzyme that catalyzes the final step in triglyceride biosynthesis by covalently attaching a long-chain fatty acyl-CoA to diacylglycerol (31, 32). Whereas DGAT2 is expressed mainly in the liver, intestine, and adipose tissue, DGAT1 is expressed in all tissues, including macrophages (31–34). To examine whether the increase in the extent of macrophage triglycerides biosynthesis in PON2-deficient

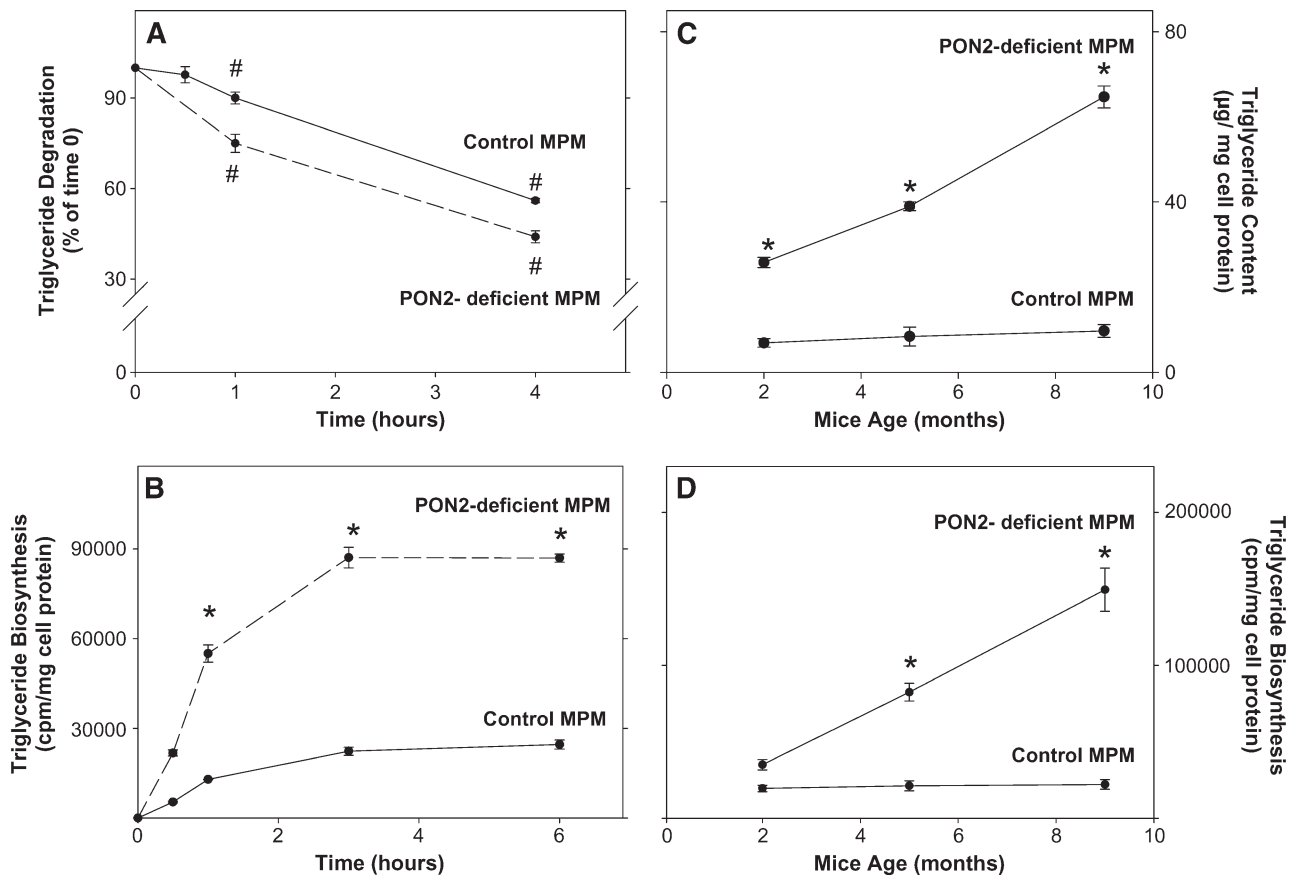


Fig. 2. Triglyceride biosynthesis in peritoneal macrophages from PON2-deficient versus control mice. MPMs were harvested from 5-month-old control (C57BL/6) mice and from age-matched PON2-deficient mice. A: MPMs (3×10^6) from both groups were incubated for 3 h at 37°C with 6 $\mu\text{Ci/ml}$ [^3H]oleate bound to fatty-acid-free BSA (2%). The cells were washed and further incubated for up to 4 h at 37°C in DMEM + 0.2% BSA. The level of cellular radiolabeled triglyceride content was determined in the lipid extract after separation of the lipids by TLC at 0 time and after 0.5, 1, and 4 h of incubation. B: MPMs (3×10^6) from both groups were incubated for up to 6 h at 37°C with 6 $\mu\text{Ci/ml}$ [^3H]oleate bound to fatty-acid-free BSA (2%). After 0.5, 1, 3, and 6 h of incubation, the cells were washed and their lipids were extracted and separated by TLC. The radioactivity in the triglyceride spots was determined by liquid scintillation counting. C, D: MPMs were harvested from PON2-deficient mice and from control mice at the ages of 2, 5, and 9 months. C: The cellular triglyceride content was determined in the TLC spots. D: The extent of triglyceride biosynthesis after 3 h of incubation was determined as described in B. Results are given as mean \pm SD of three different experiments. * $P < 0.01$ versus control MPM.

mice is related to upregulation of DGAT1, we determined microsomal DGAT1 activity in PON2-deficient and control MPM. Upon incubation of microsomes (30 μg protein/ml) for 3 h with 200 μM 1,2-dioleoyl glycerol and 135 μM oleoyl CoA, followed by triglyceride separation (by TLC), the extent of microsomal triglyceride biosynthesis in PON2-deficient MPM was significantly higher, by 4.4-fold, compared with control MPM (Fig. 3A). DGAT1 activity could have increased as a result of a posttranscriptional or a post-translational change. Thus, we next determined DGAT1 mRNA levels (as expressed by DGAT1 mRNA/GAPDH mRNA ratio) by real-time PCR (Fig. 3B) and DGAT1 protein levels (as expressed by DGAT1/ β -actin ratio) by Western blot analysis (Fig. 3C). In PON2-deficient MPM versus control MPM, similar levels of DGAT1 mRNA and DGAT1 protein were observed, suggesting that macrophage PON2 regulates DGAT1 activity and not mRNA or protein. To demonstrate that the increased DGAT1 activity in PON2-

deficient MPM indeed leads to increased triglyceride accumulation in these cells, we used the DGAT1 inhibitor oleanolic acid, which is a terpenoid (35). Direct addition of oleanolic acid (50 μM) to microsomes from PON2-deficient MPM significantly inhibited DGAT1 activity by 68% (from 2645 ± 289 μg triglyceride synthesized/mg protein to 846 ± 79 μg triglyceride synthesized/mg protein). In parallel, incubation of PON2-deficient MPM with oleanolic acid (50 μM) for 20 h at 37°C resulted in a significant reduction in the extent of triglyceride biosynthesis by 70% (Fig. 3D) compared with PON2-deficient MPM preincubated with DMSO (the solvent for oleanolic acid). Similarly, in the control MPM (harvested from C57BL/6 mice), oleanolic acid (50 μM) inhibited the extent of triglyceride biosynthesis by 75% (Fig. 3D). These results clearly indicate that, indeed, DGAT1 is responsible for triglyceride biosynthesis in PON2-deficient MPM as well as in control MPM (expressing PON2).

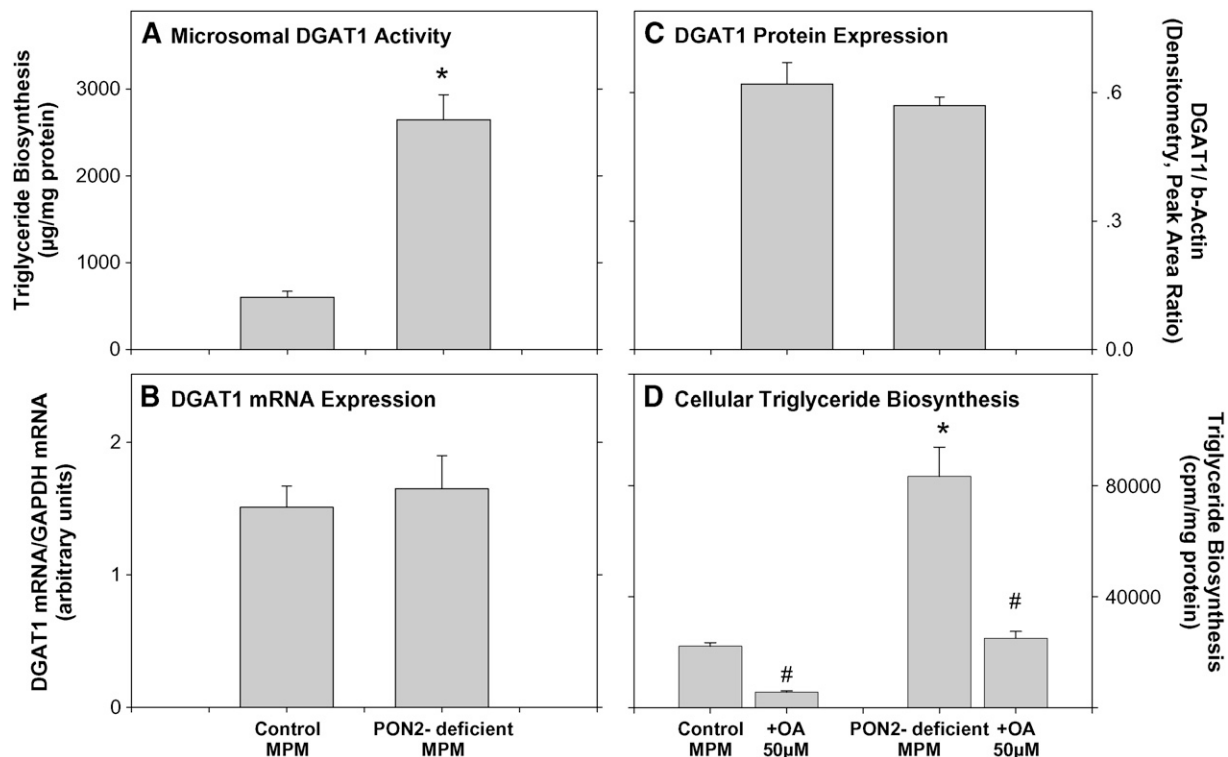


Fig. 3. DGAT1 expression in peritoneal macrophages from PON2-deficient versus control C57BL/6 mice. MPMs were harvested from 5-month-old control (C57BL/6) mice and from age-matched PON2-deficient mice. A: The microsomal fraction was separated from the MPM of both mice groups. DGAT1 activity was determined in microsomes (30 µg protein/ml) as described in Materials and Methods. B: DGAT1 mRNA levels were determined by real-time PCR using GAPDH as the normalizing gene, as described in Materials and Methods. C: DGAT1 protein levels were determined by Western blot analysis using goat polyclonal antibody to DGAT1. β-Actin was used as the normalizing protein. Densitometric analysis of the bands is shown. D: MPMs from control mice or from PON2-deficient mice were incubated for 20 h at 37°C with DMSO or with 50 µM of the DGAT1 inhibitor oleanolic acid (OA; in DMSO). Then, the cells were washed and further incubated for 3 h at 37°C with 6 µCi/ml of [³H]oleate bound to fatty-acid-free BSA (2%) in the absence or presence of 50 µM oleanolic acid. After cell wash, the cellular lipids were extracted and separated by TLC. The radioactivity in the triglyceride spots was determined by liquid scintillation counting. Results are given as mean ± SD of three different experiments. **P* < 0.01 versus control MPM. #*P* < 0.01 oleanolic-treated PON2-deficient MPM versus PON2-deficient MPM.

Direct effect of hPON2 on microsomal DGAT1 activity in PON2-deficient MPM

To further confirm the inhibitory effect of PON2 on DGAT1 activity, we added the missing PON2 to PON2-deficient MPM by transfecting them with a vector containing the hPON2 plasmid or with an empty vector (as a control). The transfected cells expressed hPON2 (inset of Fig. 4A). After transfection (48 h), we measured microsomal DGAT1 activity and cellular triglyceride content (Fig. 4A, B). Upon incubation of microsomes (30 µg protein/ml) for 3 h at 25°C with 200 µM 1,2-dioleoyl glycerol and 135 µM oleoyl CoA, followed by triglyceride separation (by TLC), the extent of triglyceride biosynthesis by microsomes from PON2-deficient MPM that were transfected with hPON2 was significantly inhibited, by 55%, compared with microsomes from control PON2-deficient MPM that were transfected with an empty vector (Fig. 4A). In parallel, cellular triglyceride content was also significantly decreased, by 53%, in hPON2-transfected MPM versus the control cells (Fig. 4B).

In addition to the above study with PON2-transfected macrophages, we also studied the direct effect of PON2 on macrophage microsomes. Addition of recombinant

PON2 at increasing concentrations (0–12 µg) to microsomes (30 µg protein) obtained from PON2-deficient mice substantially inhibited microsomal DGAT1 activity, by up to 52%, in a dose-dependent manner (Fig. 4C). The results obtained with PON2-transfected cells, as well as the direct effect of recombinant hPON2 on macrophages, clearly demonstrate that PON2 inhibits microsomal DGAT1 activity, and as a result, it attenuates triglyceride accumulation in macrophages.

Possible mechanism for PON2-mediated inhibition of DGAT1 activity

PON2 was previously shown to protect cells against oxidative stress (13, 14, 19). Increased oxidative stress (reactive oxygen species formation and cell-mediated LDL oxidation) was demonstrated also in MPM from PON2-deficient MPM versus control MPM (24). Triglycerides are easily oxidized under oxidative stress, leading to the formation of lipid peroxides. Thus, we have next measured the level of lipid peroxides (as a marker of oxidative stress) in the three systems used [PON2-deficient MPM versus control mice MPM, PON2-deficient MPM transfected with

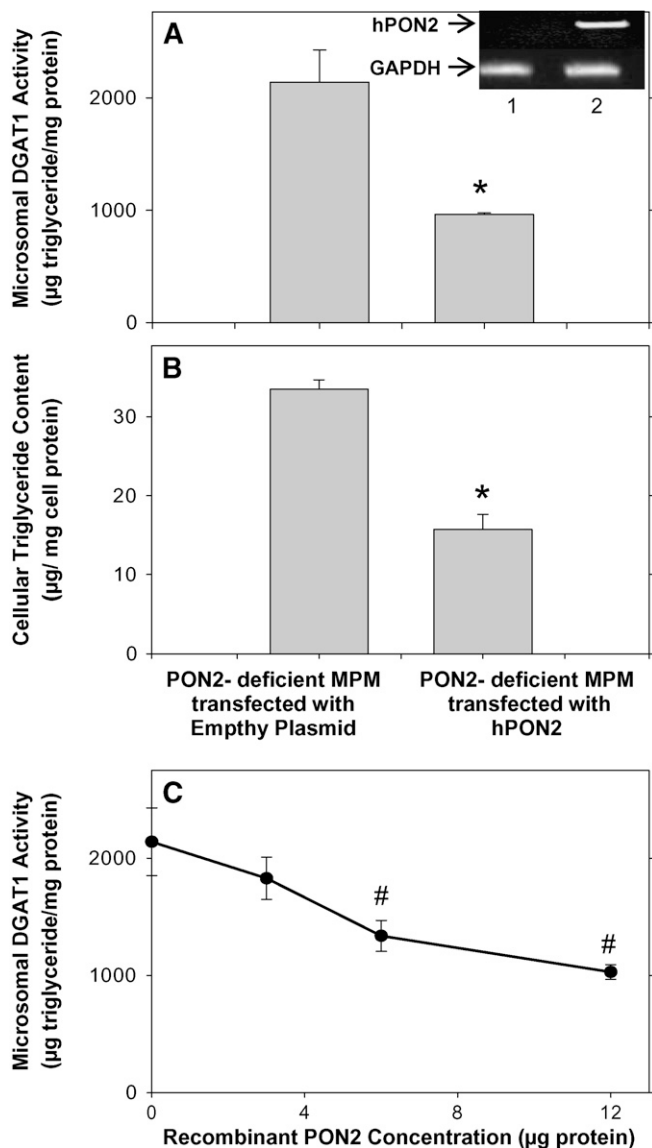


Fig. 4. The effect of hPON2 on DGAT1 activity in PON2-deficient MPM. A, B: MPMs from PON2-deficient mice at the age of 5 months were transfected with pcDNA3.1+ empty plasmid or with pcDNA3.1+ plasmid containing hPON2 for 4 h at 37°C. Microsomal DGAT1 activity (A) and cellular triglyceride content (B) were determined 48 h after transfection as described in Materials and Methods. C: The microsomes from 5-month-old PON2-deficient mice (30 µg protein) were preincubated at 37°C for 1 h with increasing concentrations (0–12 µg) of recombinant hPON2, followed by microsomal DGAT1 activity determination as described in Materials and Methods. Results are given as mean ± SD of three different experiments. **P* < 0.01 versus PON2-deficient MPMs transfected with empty plasmid. # *P* < 0.01 versus 0 concentration. The inset of A shows hPON2 and GAPDH cDNA bands. 1, PON2-deficient MPM transfected with the empty plasmid; 2, PON2-deficient MPM transfected with hPON2.

hPON2, and PON2-deficient MPM incubation with recombinant hPON2 (Fig. 5)]. We also questioned whether lipid peroxides accumulate in MPM from PON2-deficient versus control mice with the mice age in parallel to macrophage triglyceride accumulation. Indeed, the cellular lipid perox-

ides content in MPM from PON2-deficient versus control mice significantly increased with the mice age, by up to 4.8-fold, at the age of 9 months (Fig. 5A). Furthermore, in the hPON2-transfected MPM, a significant decrement in cellular lipid peroxides content, by 48%, was noted compared with the cells transfected with the empty plasmid (Fig. 5B). Similarly, in microsomes from PON2-deficient mice that were incubated with recombinant hPON2, the microsomal lipid peroxide content significantly decreased in an hPON2 dose-dependent manner, by up to 49% (Fig. 5C). These results further indicate that PON2 directly reduces the macrophage oxidative stress. To analyze the direct effect of cellular oxidative stress on DGAT1 activity, we incubated MPM from PON2-deficient mice at the age of 2 months (when they are under low oxidative stress) with either no addition, or with 2.5 mM of the free radicals generator 2,2'-amidinopropane hydrochloride (AAPH) (36). Upon cell incubation with AAPH, the MPM oxidative stress, as measured by lipid peroxide content, significantly increased by 2.2-fold (Fig. 5D) compared with the control, untreated cells. In parallel, microsomal DGAT1 activity was significantly higher, by 3.4-fold, in AAPH-treated MPM versus control MPM (Fig. 5E). In the AAPH-treated cells, the cellular triglyceride content also increased significantly, by 2.5-fold (Fig. 5F). These results clearly indicate that the increased oxidative stress in PON2-deficient MPM versus control cells leads to increased DGAT1 activity (macrophage triglyceride biosynthesis). To examine whether superoxide anions increase DGAT1 activity, we next preincubated microsomes from PON2-deficient MPM with 30 µg/ml of superoxide dismutase (SOD) for 1 h at 37°C prior to determination of microsomal DGAT1 activity. DGAT1 activity in the SOD-treated microsomes was significantly inhibited, by 40%, compared with nontreated microsomes (from 2645 ± 200 µg triglyceride synthesized/mg protein to 1587 ± 160 µg triglyceride synthesized/mg protein), suggesting that superoxide anions that were produced and accumulated in the macrophage microsomes, due to PON2 deficiency, increased cellular DGAT1 activity.

DISCUSSION

In this study, we demonstrated, for the first time, a novel anti-atherogenic protective role for macrophage PON2, i.e., inhibition of macrophage triglyceride biosynthesis, secondary to the inhibition of macrophage microsomal DGAT1 activity, which results in attenuation of macrophage triglyceride accumulation. This phenomenon possibly could be related to PON2-induced reduction in macrophage oxidative stress.

The above observations are based on studies using peritoneal macrophages (MPM) harvested from PON2-deficient (versus control C57BL/6 mice) as well as on studies performed in PON2-deficient MPM that were transfected with hPON2 and studies with MPM microsomes that were directly incubated with purified recombinant PON2.

This study demonstrated that peritoneal macrophages from PON2-deficient mice versus control mice accumulated

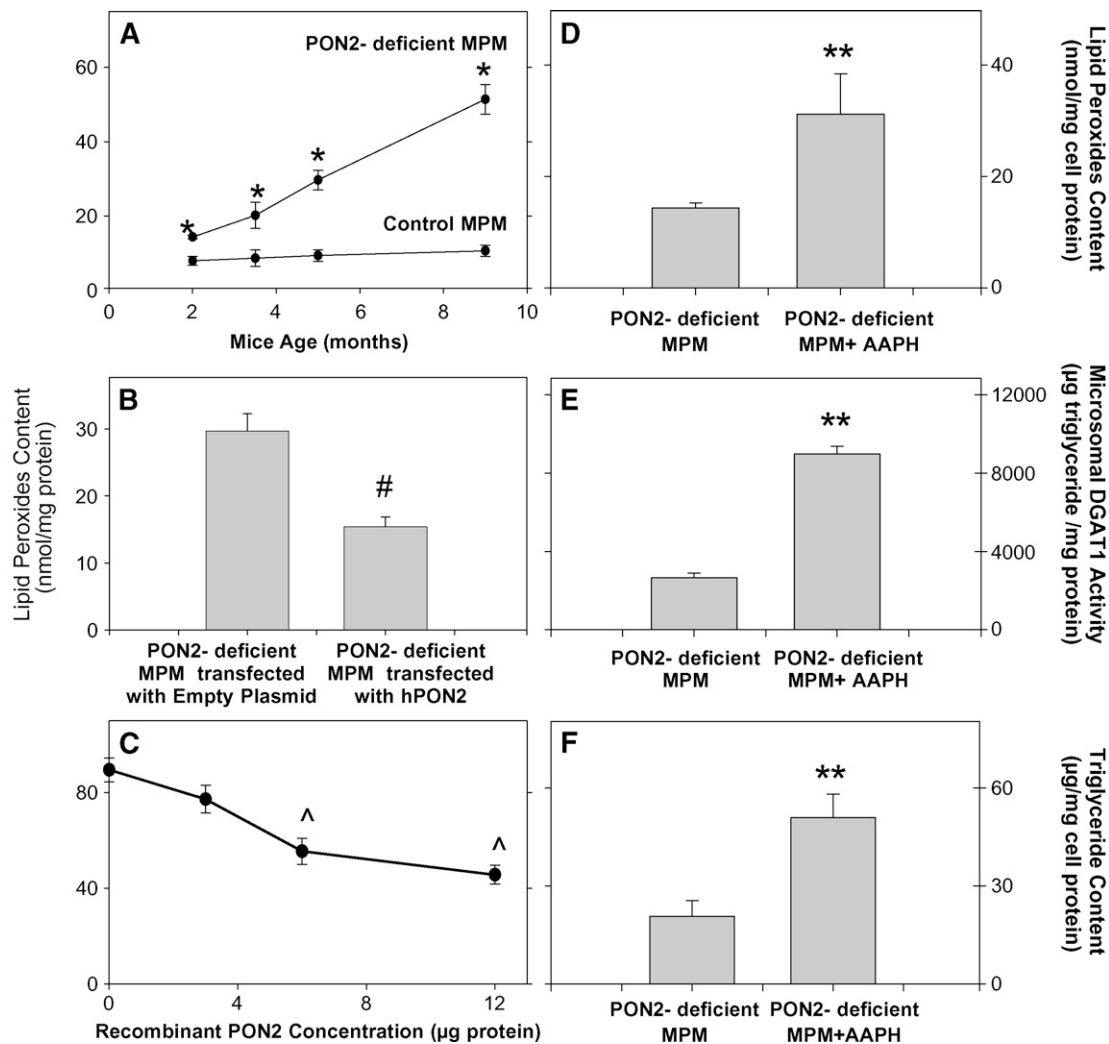


Fig. 5. The effect of oxidative stress in PON2-deficient MPM on DGAT1 activity. **A:** MPM lipid peroxide content was measured in the cell (3×10^6) lipid extract of 2-, 3.5-, 5-, and 9-month-old PON2-deficient and control (C57BL/6) mice as described in Materials and Methods. **B:** MPMs from PON2-deficient mice at the age of 5 months were transfected with pcDNA3.1+ empty plasmid or with pcDNA3.1+ plasmid containing hPON2 for 4 h at 37°C. The cellular lipid peroxides content was determined 48 h after transfection. **C:** The microsomes from 5-month-old PON2-deficient mice ($30 \mu\text{g}$ protein) were incubated at 37°C for 3 h with increasing concentrations (0–12 μg) of recombinant hPON2, followed by lipid extraction and lipid peroxide determination. **D–F:** MPMs from PON2-deficient mice at the age of 2 months were incubated overnight with no addition or in the presence of 2.5 mM of the free radical generator AAPH. **D:** Cells were then washed and the cellular lipid peroxide content was measured in the cells' lipid extract. **E:** The microsomal fraction was separated from untreated PON2-deficient MPM and from AAPH-treated cells. Microsomal DGAT1 activity was determined as described in Materials and Methods. **F:** Cellular triglyceride content was measured in the cells' lipid extract. Results are given as mean \pm SD of three different experiments. * $P < 0.01$ versus control MPM; # $P < 0.01$ versus PON2-deficient MPM transfected with empty plasmid; ^ $P < 0.01$ versus 0 concentration, ** $P < 0.01$ versus PON2-deficient MPM.


substantial amount of triglycerides but not cholesterol. This phenomenon could be related to a significant increase in the extent of cellular triglyceride biosynthesis (via DGAT1 stimulation) but not to a decreased triglyceride breakdown rate. DGAT1, which is expressed in most tissues, including macrophages (31–34), is the rate-limiting enzyme in triglyceride biosynthesis. It catalyzes the last step in the de novo triglycerides synthetic pathway, producing triglyceride from diacylglycerol and fatty acyl-CoA (31, 32). In PON2-deficient MPM versus control MPM, microsomal DGAT1 activity was significantly higher, and this could have accounted for the observed increase in triglyceride biosynthe-

sis in these cells and for the formation of triglyceride-loaded macrophages. Indeed, the DGAT1 inhibitor oleanolic acid (35) significantly decreased microsomal DGAT1 activity and, in parallel, inhibited the extent of triglyceride biosynthesis in PON2-deficient MPM. Previous studies indicated that DGAT1 is predominantly regulated posttranscriptionally (37–40). Our results clearly suggest that in PON2-deficient macrophages, although DGAT1 mRNA and protein levels were similar to those observed in control MPM, DGAT1 is activated. The increased macrophage DGAT1 activity is indeed related to PON2, as in PON2-deficient MPM that were transfected with hPON2, as well

as in microsomes that were incubated with recombinant hPON2, macrophage DGAT1 activity decreased in a PON2 dose-dependent manner.

Previous *in vitro* studies using cells overexpressing PON2, or cells in which PON2 was knocked down by small interfering RNA, demonstrated that PON2 protects cells from oxidative stress by inhibiting the formation of reactive oxygen/nitrogen species (ROS/RNS) (13, 19). Similarly, increased oxidative stress was noted in MPM from PON2-deficient versus control mice (18, 24). In this study, oxidative stress in PON2-deficient MPM was observed by the increment in lipid peroxides. These lipid peroxides could have resulted from triglyceride peroxidation under oxidative stress. Endoplasmic reticulum resident proteins are known to be most sensitive to oxidative stress (41–43), but no data are available yet on the effect of oxidative stress on DGAT1 activity. We have now clearly demonstrated that in PON2-deficient MPMs that were treated with the free radical generator AAPH, the cellular oxidative stress increased, followed by an increment in DGAT1 activity. Furthermore, reduction in oxidative stress in PON2-deficient MPM, following transfection with hPON2, or by incubating MPM microsomes with recombinant PON2 lead to the inhibition of DGAT1 activity and to a reduction in cellular triglyceride content. DGAT1 activity was inhibited by SOD, indicating the involvement of ROS in regulation of its activity. ROS that accumulate in PON2-deficient cells can increase DGAT1 activity without affecting RNA and protein expression, in a similar manner to ROS-induced activation of HMG-CoA reductase (44). Oxidative stress burden on DGAT1 by ROS could modify the substrate access to the catalytic site of the enzyme, or it can also induce structural modification of the catalytic site, thus impairing its physiological regulation by phosphorylation/dephosphorylation processes (44, 45).

The increased oxidative stress and the enhanced triglyceride accumulation in PON2-deficient MPM versus control MPM could be relevant also to arterial macrophages. Indeed, in the mice aorta, we observed increased levels of lipid peroxides and triglycerides, but not cholesterol (data not shown). All the above phenomena could account for the enhanced atherosclerosis development in PON2-deficient mice observed under atherogenic diet (18).

In conclusion, this study shows that PON2 protects macrophages from cellular triglyceride accumulation and foam cell formation by regulating DGAT1 activity, which appears to be sensitive to the oxidative state. The above phenomena could lead to PON2-mediated attenuation of atherosclerosis development. 

REFERENCES

1. Carmena, R., P. Duriez, and J. C. Fruchart. 2004. Atherogenic lipoprotein particles in atherosclerosis. *Circulation*. **109**: III2–III7.
2. Cullen, P. 2000. Evidence that triglycerides are an independent coronary heart disease risk factor. *Am. J. Cardiol*. **86**: 943–949.
3. Aviram, M., and M. Rosenblat. 2004. Paraoxonases 1, 2 and 3, oxidative stress, and macrophage foam cell formation during atherosclerosis development. *Free Radic. Biol. Med.* **37**: 1304–1316.
4. Tiwari, R. L., Y. Singh, and M. K. Barthwal. 2008. Macrophages: an elusive yet emerging therapeutic target of atherosclerosis. *Med. Res. Rev.* **28**: 483–544.
5. Lusis, A. J. 2000. Atherosclerosis. *Nature*. **407**: 233–241.
6. Lang, P. D., and W. Jr Insull. 1970. Lipid droplets in atherosclerotic fatty streaks of human aorta. *J. Clin. Invest.* **49**: 1479–1488.
7. Lundberg, B. 1985. Chemical composition and physical state of lipid deposits in atherosclerosis. *Atherosclerosis*. **56**: 93–110.
8. Mattsson, L., H. Johansson, M. Ottosson, G. Bondjers, and O. Wilklund. 1993. Expression of lipoprotein lipase mRNA and secretion in macrophages isolated from human atherosclerotic aorta. *J. Clin. Invest.* **92**: 1759–1765.
9. Botham, K. M., E. H. Moore, C. D. Pascale, and F. Bejta. 2007. The induction of macrophage foam cell formation by chylomicrons remnants. *Biochem. Soc. Trans.* **35**: 454–458.
10. Napolitano, M., M. Avella, K. M. Botham, and E. Bravo. 2003. Chylomicrons remnant induction of lipid accumulation in J774 A.1 macrophages is associated with up-regulation of triacylglycerol synthesis which is not dependent on oxidation of the particles. *Biochim. Biophys. Acta.* **1631**: 255–264.
11. Aronis, A., Z. Madar, and O. Tirosh. 2005. Mechanism underlying oxidative stress-mediated lipotoxicity: exposure of J774.2 macrophages to triacylglycerols facilitates mitochondrial reactive oxygen species production and cellular necrosis. *Free Radic. Biol. Med.* **38**: 1221–1230.
12. Draganov, D. I., J. F. Teiber, A. Speelman, Y. Osawa, R. Sunahara, and B. N. La Du. 2005. Human paraoxonases (PON1, PON2, and PON3) are lactonases with overlapping and distinct substrate specificities. *J. Lipid Res.* **46**: 1239–1247.
13. Ng, C. J., D. J. Wadleigh, A. Gangopadhyay, S. Hama, V. R. Grijalva, M. Navab, A. M. Fogelman, and S. T. Reddy. 2001. Paraoxonase-2 is a ubiquitously expressed protein with antioxidant properties and is capable of preventing cell-mediated oxidative modification of low density lipoprotein. *J. Biol. Chem.* **276**: 44444–44449.
14. Rosenblat, M., D. Draganov, C. E. Watson, C. L. Bisgaier, B. N. La Du, and M. Aviram. 2003. Mouse macrophage paraoxonase 2 activity is increased whereas cellular paraoxonase 3 activity is decreased under oxidative stress. *Arterioscler. Thromb. Vasc. Biol.* **23**: 468–474.
15. Rosenblat, M., T. Hayek, K. Hussein, and M. Aviram. 2004. Decreased macrophage paraoxonase 2 expression in patients with hypercholesterolemia is the result of their increased cellular cholesterol content: effect of atorvastatin therapy. *Arterioscler. Thromb. Vasc. Biol.* **24**: 175–180.
16. Fortunato, G., M. D. Di Taranto, U. M. Bracale, L. Del Guercio, F. Carbone, C. Mazzaccara, A. Morgante, F. P. D'Armiento, M. D'Armiento, M. Porcellini, et al. 2008. Decreased paraoxonase-2 expression in human carotids during the progression of atherosclerosis. *Arterioscler. Thromb. Vasc. Biol.* **28**: 594–600.
17. Ng, C. J., S. Y. Hama, N. Bourquard, M. Navab, and S. T. Reddy. 2006. Adenovirus mediated expression of human paraoxonase 2 protects against the development of atherosclerosis in apolipoprotein E-deficient mice. *Mol. Genet. Metab.* **89**: 368–373.
18. Ng, C. J., N. Bourquard, V. R. Grijalva, S. Hama, D. M. Shih, M. Navab, A. M. Fogelman, A. J. Lusis, S. Young, and S. T. Reddy. 2006. Paraoxonase-2 deficiency aggravates atherosclerosis in mice despite lower apolipoprotein-B-containing lipoproteins: anti-atherogenic role for paraoxonase-2. *J. Biol. Chem.* **281**: 29491–29500.
19. Horke, S., I. Witte, P. Wilgenbus, M. Krüger, D. Strand, and U. Förstermann. 2007. Paraoxonase-2 reduces oxidative stress in vascular cells and decreases endoplasmic reticulum stress-induced caspase activation. *Circulation*. **115**: 2055–2064.
20. Shiner, M., B. Fuhrman, and M. Aviram. 2006. A biphasic U-shape effect of cellular oxidative stress on the macrophage anti-oxidant paraoxonase 2 (PON2) enzymatic activity. *Biochem. Biophys. Res. Commun.* **349**: 1094–1099.
21. Shiner, M., B. Fuhrman, and M. Aviram. 2004. Paraoxonase 2 (PON2) expression is upregulated via a reduced-nicotinamide-adenine-dinucleotide-phosphate (NADPH)-oxidase-dependent mechanism during monocytes differentiation into macrophages. *Free Radic. Biol. Med.* **37**: 2052–2063.
22. Shiner, M., B. Fuhrman, and M. Aviram. 2007. Macrophage paraoxonase 2 (PON2) expression is up-regulated by pomegranate juice phenolic anti-oxidants via PPAR gamma and AP-1 pathway activation. *Atherosclerosis*. **195**: 313–321.
23. Shiner, M., B. Fuhrman, and M. Aviram. 2007. Macrophage paraoxonase 2 (PON2) expression is upregulated by unesterified cholesterol through activation of the phosphatidylinositol 3-kinase (PI3K) pathway. *Biol. Chem.* **388**: 1353–1358.

24. Fuhrman, B., J. Khateeb, M. Shiner, O. Nitzan, R. Karry, N. Volkova, and M. Aviram. 2008. Urokinase plasminogen activator upregulates paraoxonase 2 expression in macrophages via an NADPH oxidase-dependent mechanism. *Arterioscler. Thromb. Vasc. Biol.* **28**: 1361–1367.
25. Coleman, R., T. Hayek, S. Kiar, and M. Aviram. 2006. A mouse model for human atherosclerosis: long-term histopathological study of lesion development in the aortic arch of apolipoprotein E-deficient E (0) mice. *Acta Histochem.* **108**: 415–424.
26. Neuhuber, B., D. I. Huang, M. P. Daniels, and C. E. Torgan. 2002. High efficiency transfection of primary skeletal muscle cells with lipid-based reagents. *Muscle Nerve.* **26**: 136–140.
27. Hellgren, L., V. Drvota, R. Pieper, S. Enoksson, P. Biornberg, K. B. Islam, and C. Sylven. 2000. Highly efficient cell-mediated gene transfer using non-viral vectors and Fugene6: in vitro and in vivo studies. *Cell. Mol. Life Sci.* **57**: 1326–1333.
28. Lowry, O. H., N. J. Rosebrough, A. L. Farr, and R. J. Randall. 1951. Protein measurement with the Folin phenol reagent. *J. Biol. Chem.* **193**: 265–275.
29. Vaziri, N. D., C. H. Kim, D. Phan, S. Kim, and K. Liang. 2004. Up-regulation of hepatic acylCoA:diacylglycerol acyltransferase-1 (DGAT1) expression in nephrotic syndrome. *Kidney Int.* **66**: 262–267.
30. El-Saadani, M., N. Esterbauer, M. El-Sayed, M. Goher, A. Y. Nassar, and G. Jurgens. 1989. Spectrophotometric assay for lipid peroxides in serum lipoproteins using commercially available reagent. *J. Lipid Res.* **30**: 627–630.
31. Farese, R. V., Jr., S. Cases, and S. J. Smith. 2000. Triglyceride synthesis: insights from the cloning of diacylglycerol acyltransferase. *Curr. Opin. Lipidol.* **11**: 229–234.
32. Cases, S., S. J. Smith, Y.W. Zheng, H. M. Myers, S. R. Lear, E. Sande, S. Nivak, C. Collins, C. B. Welch, A. J. Lusis, et al. 1998. Identification of a gene encoding an acyl CoA:diacylglycerol acyltransferase, a key enzyme in triacylglycerol synthesis. *Proc. Natl. Acad. Sci. USA.* **95**: 13018–13023.
33. Cases, S., S. J. Stone, P. Zhou, E. Yen, B. Tow, K. D. Lardizabal, T. Voelker, and R. V. Farese, Jr. 2001. Cloning of DGAT2: a second mammalian diacylglycerol acyltransferase, and related family members. *J. Biol. Chem.* **276**: 38870–38876.
34. Moore, E. H., M. Napolitano, A. Prosperi, M. Avella, K. E. Suckling, E. Bravo, and K. M. Botham. 2003. Incorporation of lycopene into chylomicron remnant-like particles enhances their induction of lipid accumulation in macrophages. *Biochem. Biophys. Res. Commun.* **312**: 1216–1219.
35. Dat, N. T., X. F. Cai, M. C. Rho, H. S. Lee, K. Bae, and Y. H. Kim. 2005. The inhibition of diacylglycerol acyltransferase by terpenoids from *Youngia koidzumiana*. *Arch. Pharm. Res.* **28**: 164–168.
36. Frei, B., R. Stocker, and B. N. Ames. 1988. Antioxidant defenses and lipid peroxidation in human blood plasma. *Proc. Natl. Acad. Sci. USA.* **85**: 9748–9752.
37. Lehner, R., and A. Kuis. 1996. Biosynthesis of triacylglycerol. *Prog. Lipid Res.* **35**: 169–201.
38. Coleman, R. A., and D. P. Lee. 2004. Enzymes of triacylglycerol synthesis and their regulation. *Prog. Lipid Res.* **43**: 134–176.
39. Yu, Y. H., Y. Zhang, P. Olelkers, S. L. Sturley, D. J. Rader, and H. N. Ginsberg. 2002. Posttranscriptional control of the expression and function of diacylglycerol acyltransferase-1 in mouse adipocytes. *J. Biol. Chem.* **277**: 50876–50884.
40. Casaschi, A., G. K. Maiyoh, K. Adeli, and A. G. Theriault. 2005. Increased diacylglycerol acyltransferase activity is associated with triglyceride accumulation in tissues of diet-induced insulin-resistant hyperlipidemic hamsters. *Metabolism.* **54**: 403–409.
41. Van Der Vlies, D., M. Makkinje, A. Jansens, I. Braakman, A. J. Verkleij, K. W. A. Wirtz, and J. A. Post. 2003. Oxidation of ER resident proteins upon oxidative stress: effects of altering cellular redox/antioxidant status and implications for protein maturation. *Antioxid. Redox Signal.* **5**: 381–387.
42. Kaplán, P., M. Doval, Z. Majerová, J. Lehotský, and P. Racay. 2000. Iron-induced lipid peroxidation and protein modification in endoplasmic reticulum membranes. Protection by stobadine. *Int. J. Biochem. Cell Biol.* **32**: 539–547.
43. Van Der Vlies, D., E. H. W. Pap, J. A. Post, J. E. Celis, and K. W. A. Wirtz. 2002. Endoplasmic reticulum resident proteins of normal human dermal fibroblasts are the major targets for oxidative stress induced by hydrogen peroxide. *Biochem. J.* **366**: 825–830.
44. Pallottini, V., C. Martini, A. Pascolini, G. Cavallini, Z. Gori, E. Bergamini, S. Incerpi, and A. Trentalance. 2005. 3-Hydroxy-3-methylglutaryl coenzyme A reductase deregulation and age-related hypercholesterolemia: a new role for ROS. *Mech. Ageing Dev.* **126**: 845–851.
45. Pallottini, V., C. Martini, G. Cavallini, E. Bergamini, K. J. Mustard, D. G. Hardie, and A. Trentalance. 2007. Age-related HMG-CoA reductase deregulation depends on ROS-induced p38 activation. *Mech. Ageing Dev.* **128**: 688–695.